

GRAPHINE: GRAPH IMPORTANCE PROPAGATION FOR INTERPRETABLE DRUG RESPONSE PREDICTION

Yoshitaka Inoue

Department of Computer Science and Engineering
University of Minnesota
Minneapolis, MN, USA
Computational Biology Branch, National Library of Medicine
Developmental Therapeutics Branch, National Cancer Institute
Bethesda, MD, USA
inoue019@umn.edu

Tianfan Fu

Department of Computer Science,
Nanjing University
Nanjing, Jiangsu, China
futianfan@gmail.com

Augustin Luna

Computational Biology Branch, National Library of Medicine
Developmental Therapeutics Branch, National Cancer Institute
Bethesda, MD, USA
augustin@nih.gov

ABSTRACT

Explainability is necessary for many tasks in biomedical research. Recent explainability methods have focused on attention, gradient, and Shapley value. These do not handle data with strong associated prior knowledge and fail to constrain explainability results based on known relationships between predictive features.

We propose GraphPINE, a graph neural network (GNN) architecture leveraging domain-specific prior knowledge to initialize node importance optimized during training for drug response prediction. Typically, a manual post-prediction step examines literature (i.e., prior knowledge) to understand returned predictive features. While node importance can be obtained for gradient and attention after prediction, node importance from these methods lacks complementary prior knowledge; GraphPINE seeks to overcome this limitation. GraphPINE differs from other GNN gating methods by utilizing an LSTM-like sequential format. We introduce an importance propagation layer that unifies 1) updates for feature matrix and node importance and 2) uses GNN-based graph propagation of feature values. This initialization and updating mechanism allows for informed feature learning and improved graph representation.

We apply GraphPINE to cancer drug response prediction using drug screening and gene data collected for over 5,000 gene nodes included in a gene-gene graph with a drug-target interaction (DTI) graph for initial importance. The gene-gene graph and DTIs were obtained from curated sources and weighted by article count discussing relationships between drugs and genes. GraphPINE achieves a PR-AUC of 0.894 and ROC-AUC of 0.796 across 952 drugs. Code is available at <https://anonymous.4open.science/r/GraphPINE-40DE>.

1 INTRODUCTION

Drug response prediction (DRP) is an open research challenge in personalized medicine and drug discovery. Work in this research area seeks to improve treatment outcomes and reduce adverse effects. However, the complex interplay between drug compounds and cellular entities makes this task challenging. Traditional approaches often fail to capture the intricate network of interactions that influence drug response, leading to suboptimal predictions with limited interpretability. Despite recent advancements, current DRP methods face challenges such as data heterogeneity, limited sample sizes, and the need for multi-omics integration (Azuaje, 2017; Lu, 2018; Vamathevan et al., 2019).

Greater data availability combined with algorithmic improvements have led to an increase in machine learning (ML) techniques in this research area. GNNs have emerged as a promising approach due to their ability to model complex relational data (Kipf & Welling, 2016). Recent GNN variants, such as Graph Transformer Networks (Yun et al., 2019) and Graph Diffusion Networks (Klicpera et al., 2019), have shown promise in capturing complex, long-range dependencies in biological networks. However, these advanced architectures often come at the cost of increased complexity and reduced interpretability. This leads to two main limitations in existing GNN models for DRP. First, many models do not incorporate known biological information, such as DTI. This omission can lead to predictions that, while accurate, may not align with known biological mechanisms. Second, the “black box” nature of many deep learning models makes it difficult for researchers and clinicians to understand and trust the predictions. This lack of interpretability is a significant barrier to adopting these models for furthering understanding of drug mechanisms.

While some attempts have been made to incorporate biological priors into GNNs (Zitnik et al., 2018) or improve interpretability (Ying et al., 2019), no existing method addresses both challenges in the context of DRP. To address these limitations, we introduce GraphPINE (**Graph Propagating Importance Network for Explanation**), a novel GNN approach combining the predictive power of deep learning with biologically informed feature importance propagation and interpretability.

The key innovation of GraphPINE lies in its Importance Propagation (IP) Layer, which updates and propagates gene importance scores across the network during the learning process. This mechanism allows GraphPINE to:

1. Integrate known DTI information with the underlying gene network structure, ensuring the model’s predictions are grounded in known biological interactions.
2. Capture drug-gene interactions with N-hops GNN layers, providing a more comprehensive view of drug influence on the gene network.
3. Generate interpretable visualizations of gene-gene interactions under the drug treatment, offering new perspectives on potential drug action mechanisms.

2 RELATED WORKS

2.1 DRUG RESPONSE PREDICTION

DRP refers to the process of forecasting how a particular drug will affect the viability of a biological system based on various data inputs such as genomic information and molecular structures (Adam et al., 2020). The goal is to predict the drug sensitivity, which can aid in personalized medicine, allowing for more targeted treatments for patients.

Several notable models have emerged: Li et al. (2019) developed DeepDSC combining an autoencoder for gene expression to obtain hidden embeddings, which are then used as input to a feed-forward network along with drug fingerprint embeddings. Lao et al. (2024) implemented the DeepAEG, including transformer for SMILES and attention for multi-omics data (e.g., mutation, gene expression).

2.2 GRAPH NEURAL NETWORKS IN COMPUTATIONAL BIOLOGY

GNNs have emerged as a powerful tool for modeling complex biological systems. Huang et al. (2021) utilized GNNs for side effect prediction with drug-drug interaction networks. GNNs have also been used for molecular property prediction, showcasing the potential of GNNs in cheminformatics (Fu et al., 2021b). For the DRP, GraphDRP (Nguyen et al., 2021) integrates gene expression and protein-protein interaction networks, while MOFGCN (Peng et al., 2021) combines multi-omics data.

2.3 EXPLAINABLE AI IN BIOLOGICAL APPLICATIONS

As ML models become complex, there is a growing need for interpretability, especially in biomedical applications where understanding the rationale behind predictions is fundamental for clinical research. Explainable AI methods can be categorized into three main types:

1. **Gradient-based methods:** These techniques utilize gradient information to highlight important features. For example, Grad-CAM (Selvaraju et al., 2020) generates visual explanations

for decisions made by convolutional neural networks. Fu et al. (2021a) produces molecular substructure-level gradient to provide interpretability for drug design.

2. **Attention-based methods:** These approaches leverage attention coefficients to identify relevant inputs. Abnar & Zuidema (2020) propose attention flow to quantify the information propagation through self-attention layers, improving the interpretability of the Transformer. For DRP, Inoue et al. (2024) employs Graph Attention Network (GAT) (Veličković et al., 2017) on a heterogeneous network of proteins, cell lines, and drugs, offering interpretability through attention coefficients.
3. **Shapley value-based methods:** SHapley Additive exPlanations (SHAP) (Lundberg & Lee, 2017; Wang et al., 2024) assigns importance values to input features based on game theory principles, providing a unified measure of feature contributions to model predictions.

GraphPINE is related to the attention-based methods but with key distinctions. Unlike typical attention mechanisms assigning importance to edges, GraphPINE uses DTI information to initialize node importance scores. It propagates this importance throughout the learning process along with the graph structure. This approach incorporates biological knowledge, thereby enhancing interpretability.

2.4 INFORMATION PROPAGATION IN NEURAL NETWORKS

Shrikumar et al. (2017) proposed DeepLIFT (Deep Learning Important FeaTures). This method computes importance scores, capturing non-linear dependencies that might be missed by other approaches. DeepLIFT addresses the limitations of traditional gradient-based methods by considering the difference from a reference input. This approach offers a more nuanced understanding of feature contributions and provides more interpretable explanations of model outputs.

More recently, Abnar & Zuidema (2020) introduced Attention Flow, a method designed for Transformer models. This approach models the propagation of attention through the layers of a Transformer, quantifying how information flows from input tokens to output tokens. Attention Flow provides a more accurate measure of token relationships compared to raw attention weights, offering insights into how Transformer models process and utilize information across their multiple attention layers.

These methods can all be viewed as specialized forms of information propagation. In each case, the “information” being propagated represents the relevance, importance, or attention associated with different components of the network. These approaches demonstrate how the concept of information propagation can be leveraged to enhance the interpretability of complex neural network models, offering valuable insights into their decision-making processes across various network architectures.

2.5 IMPORTANCE GATING WITH GNNS

Recent studies have proposed different approaches for incorporating gating mechanisms into GNNs. Two notable examples are Event Detection GCN (Lai et al., 2020) and CID-GCN (Zeng et al., 2021).

Event detection is a natural language processing (NLP) task aiming to identify specific events (e.g., accidents) from documents. Event Detection GCN implements a gating mechanism utilizing trigger candidate information (e.g., potential event-indicating words: “attacked”) to filter noise from hidden vectors. The model incorporates gate diversity across layers and leverages syntactic importance scores from dependency trees, which represent grammatical relationships between words in sentences.

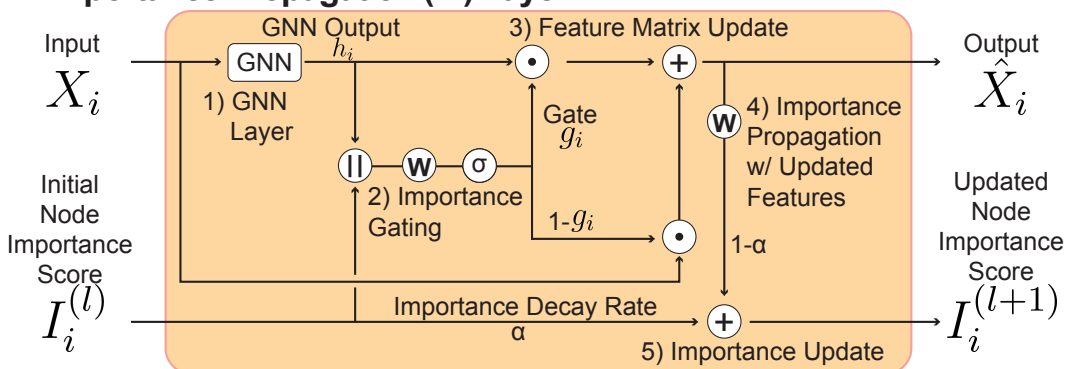
CID-GCN, designed for chemical-disease relation extraction, constructs a heterogeneous graph with mentions (representing specific entity occurrences), sentences (containing the textual context), and entities (normalizing multiple mentions) nodes. The model employs gating mechanisms to address the over-smoothing problem and enables effective information propagation between distant nodes.

GraphPINE advances these concepts through two key ideas. First, it introduces a novel approach to importance scoring by leveraging domain-specific prior knowledge for initialization rather than relying solely on previous hidden states. Second, it implements a unified importance score updating mechanism through graph learning, departing from the context-based or two-step gating methods.

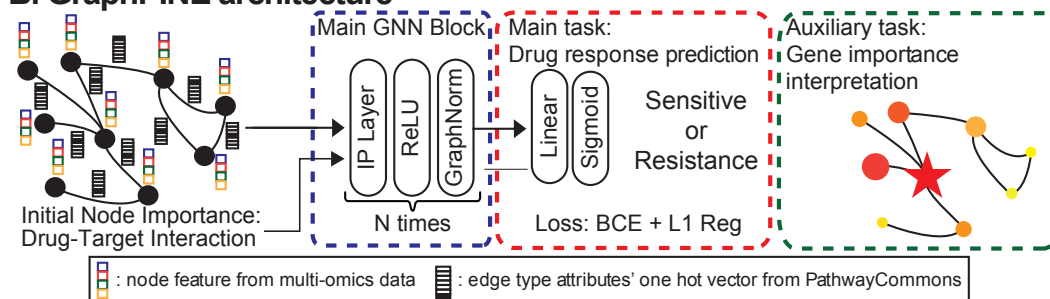
3 METHODS

This section presents the GraphPINE model, including data preprocessing, network construction, and the model architecture. GraphPINE is a GNN architecture designed for accurate and interpretable

A. Importance Propagation (IP) Layer



B. GraphPINE architecture



C. How to create the graph structure

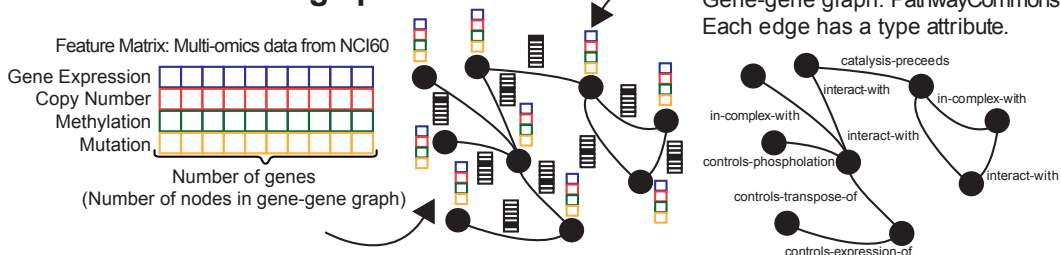


Figure 1: Overview of GraphPINE Components. (A) Importance Propagation (IP) Layer: This illustrates the key components of the IP Layer in the GraphPINE model, including the GNN, importance gating, feature updates with residual connections, importance propagation, and updates. The symbols represent the following operations: σ is the activation function, \odot is element-wise multiplication, \times is multiplication, $+$ is addition, W denotes weighted calculation with bias, \parallel represents concatenation, and α is a hyperparameter for controlling importance. (B) GraphPINE architecture. (C) Data Creation Overview: The model integrates multi-omics data (gene expression, copy number, methylation, mutation) from NCI60 (Shoemaker, 2006) with gene-gene interaction networks from PathwayCommons (Cerami et al., 2010; Rodchenkov et al., 2019). Each edge has attributes such as “interact-with”, which are converted into one-hot vectors for edge attribution.

DRP, leveraging multi-omics data (e.g., gene expression, copy number variation, methylation, and mutation information), along with known biological interactions to provide comprehensive insights into drug-target relationships, as illustrated in Figure 1.

3.1 DATA PREPROCESSING AND NETWORK CONSTRUCTION

We integrated three key datasets to generate a gene-gene interaction network with initial importance weights. First, we incorporated a gene-gene interaction network from PathwayCommons as our base graph structure. Second, we collected multi-omics profiles from NCI-60 cell lines to serve as node features. Third, we obtained drug-target interactions from five databases: CTD (Davis et al.,

2023), DrugBank (Wishart et al., 2018), DGIdb (Freshour et al., 2021), STITCH (Szklarczyk et al., 2021), and KIBA (Tang et al., 2014), which we used to establish initial node importance weights. We selected genes based on their variance, network centrality, and drug-target interaction frequency. Comprising 5,181 genes and 630,632 interactions. In addition, network edge types were encoded as one-hot vectors (see Appendix A.1).

Gene expression data was normalized using TPM, Log2 transformation, and winsorization. Each gene in each cell line was represented by a 4-dimensional feature vector combining all multi-omics data. DTI scores were calculated from multiple databases, encompassing both direct physical binding between drugs and targets, as well as their indirect associations.

Let $S_{dti}(d_i, g_j)$ be the initial importance score for drug d_i and gene g_j . We normalized these scores to a range of $[0.5, 1]$:

$$\begin{aligned} \log_count &= \log(1 + \text{PubMed ID_count}) \\ S_{dti}(d_i, g_j) &= 0.5 + 0.5 \times \frac{\log_count - \min(\log_count)}{\max(\log_count) - \min(\log_count)}. \end{aligned} \quad (1)$$

Here, \log_count refers to the log-transformed PubMed ID counts, where PubMed ID_count represents the number of papers retrieved from PubMed ESearch (Sayers, 2009) using the query that searches for co-mentions by combining drug name and gene name. d_i and g_j denote specific drugs and genes. The 0.5 is added to distinguish the genes that are in databases, but they don't have the literature information. Therefore, the range of $S_{dti}(d_i, g_j)$ is $S_{dti}(d_i, g_j) \in \{0\} \cup [0.5, 1]$.

3.2 GRAPHFINE MODEL ARCHITECTURE

The GraphFINE model predicts drug response and learns gene importance using a gene interaction network $G = (V, E)$ with node features $X \in \mathbb{R}^{|V| \times d}$; edge features $E_{attr} \in \mathbb{R}^{|E| \times f}$, and importance scores $I \in \mathbb{R}^{|V|}$. The model outputs a predicted drug response $\hat{y} \in \mathbb{R}$ and updated importance score $I' \in \mathbb{R}^{|V|}$, utilizing edge-aware GNN architectures (i.e., Graph Attention Network (GAT) (Veličković et al., 2017), Graph Transformer (GT) (Yun et al., 2019), and Graph Isomorphism Network with Edge features (GINE) (Hu et al., 2019)).

3.2.1 IMPORTANCE PROPAGATION LAYER

The Importance Propagation Layer (IP Layer) is a key component that processes and updates node features while considering their importance scores. The layer operates through five main steps:

1. Apply TransformerConv to process node features. This step transforms the input node features using graph topology:

$$\mathbf{h}_i = \text{TransformerConv}(\mathbf{x}_i, \text{edge_index}, \text{edge_attr}) \quad (2)$$

2. Generate gate using GT output and importance scores. The gate controls information flow based on node importance:

$$\mathbf{g}_i = \sigma(\mathbf{W}_g[\mathbf{h}_i \| I_i] + \mathbf{b}_g) \quad (3)$$

where σ is the sigmoid function and $\|$ denotes concatenation.

3. Update node features using a gating mechanism that combines original and transformed features:

$$\hat{\mathbf{x}}_i = \mathbf{g}_i \odot \mathbf{h}_i + (1 - \mathbf{g}_i) \odot \mathbf{x}_i \quad (4)$$

where \odot represents element-wise multiplication.

4. Propagate importance scores through the network using a learnable transformation:

$$I'_i = \mathbf{W}_p \hat{\mathbf{x}}_i + b_p \quad (5)$$

5. Update and normalize importance scores. First, update scores using a decay mechanism:

$$I_i^{(l+1)} = \alpha I_i^{(l)} + (1 - \alpha) I'_i \quad (6)$$

Then, normalize and threshold the scores:

$$I_i^{\text{norm}} = \frac{I_i - \min(I)}{\max(I) - \min(I)}, \quad I_i^{\text{final}} = \begin{cases} I_i^{\text{norm}} & \text{if } I_i^{\text{norm}} \geq \theta \\ 0 & \text{otherwise} \end{cases} \quad (7)$$

where θ is the importance threshold that determines which nodes are considered significant.

3.2.2 MODEL ARCHITECTURE

The model consists of three stacked IP Layers with GraphNorm, Dropout, and ReLU between layers. The final prediction is computed as follows:

$$p = \sigma \left(\mathbf{W}f \left(\frac{1}{|V|} \sum_{v \in V} \mathbf{h}_v^{(L)} \right) + b_f \right) \quad (8)$$

where p is the positive class probability and $\mathbf{h}_v^{(L)}$ is the final node representation. The loss function combines binary cross entropy (BCE) and importance regularization:

$$\mathcal{L} = \mathcal{L}_{\text{BCE}} + w_{\text{imp}} \cdot \mathcal{L}_{\text{imp}} \quad (9)$$

where \mathcal{L}_{imp} is L1 regularization on importance scores.

4 EXPERIMENTS

4.1 DATASET

We processed the NCI-60 dataset (Shoemaker, 2006) using rcellminer (Luna et al., 2016), applying a threshold of -4.595 to log-transformed IC50 (50% inhibitory concentration) values to initially achieve a balanced 50:50 drug sensitive/resistance labels ratio. After selecting drugs with NSC (National Service Center number) identifiers, the final dataset comprised 53,852 entries (36,171 positive, 17,681 negative). For zero-shot prediction, we split the data using 70% cell lines and 60% drugs for training/validation (571 drugs, 42 cell lines) and the rest for testing (381 drugs, 18 cell lines). This resulted in 18,067 training, 4,516 validation, and 6,525 test samples.

4.2 PREDICTION PERFORMANCE

To evaluate GraphPINE, we compared it against several baseline methods, including five traditional ML approaches, two current research methods, and 3 GNNs without an IP layer. Table 1 presents the performance metrics for each method, averaged over five independent runs.

Our GraphPINE model, particularly the GT variant, demonstrates superior performance across multiple metrics. Given the imbalanced nature of our dataset, we place particular emphasis on the PR-AUC and ROC-AUC scores as the most critical evaluation metrics. Notably, GraphPINE (GT) achieves the highest PR-AUC (0.894) and ROC-AUC (0.796), underscoring its effectiveness in handling imbalanced data. While DeepDSC shows higher accuracy (0.751) and precision (0.807), GraphPINE (GT)’s balanced performance across multiple metrics indicates its robust ability to effectively discriminate between classes.

MOFGCN exhibits a performance pattern with a high specificity (0.901) but poor performance across other metrics (ROC-AUC: 0.492, PR-AUC: 0.666, Accuracy: 0.355). This suggests that while the model excels at identifying resistance, it does so at the expense of overall classification performance, indicating a highly imbalanced prediction behavior that limits its utility.

The ablation study demonstrates the significant impact of the IP layer across all architectures. The GT variant achieves the best performance with PR-AUC of 0.894 and ROC-AUC of 0.796, representing improvements of 2.29% and 2.74% from its baseline scores of 0.874 and 0.774, respectively. The GAT architecture exhibits notable enhancements, with PR-AUC increasing by 2.74% (from 0.868 to 0.892) and ROC-AUC by 4.04% (from 0.758 to 0.789). Most remarkably, the GINE architecture shows the most substantial improvement, with PR-AUC increasing by 12.29% (from 0.794 to 0.891) and ROC-AUC by 5.36% (from 0.750 to 0.790), demonstrating the IP layer’s effectiveness in enhancing model performance.

It is worth noting that all variants of GraphPINE (GINE, GAT, and GT) show low standard deviations across runs, indicating the stability and reliability of our proposed method. This consistency is valuable when dealing with imbalanced datasets, as it suggests that our model’s performance is robust across different data splits and initializations.

	Methods	Explainability	ROC-AUC (\uparrow)	PR-AUC (\uparrow)	Accuracy (\uparrow)	Precision (\uparrow)	Specificity (\uparrow)
Baseline	RF	Feature Importance	0.788 (± 0.001)	0.892 (± 0.002)	0.716 (± 0.002)	0.726 (± 0.002)	0.632 (± 0.003)
	LightGBM	Feature Importance	0.790 (± 0.000)	0.870 (± 0.000)	0.747 (± 0.000)	0.769 (± 0.000)	0.457 (± 0.000)
	MLP	-	0.750 (± 0.010)	0.838 (± 0.006)	0.710 (± 0.004)	0.721 (± 0.009)	0.271 (± 0.051)
	MPNN	-	0.792 (± 0.013)	0.892 (± 0.006)	0.728 (± 0.009)	0.726 (± 0.011)	0.571 (± 0.044)
	GCN	-	0.766 (± 0.019)	0.872 (± 0.010)	0.710 (± 0.021)	0.710 (± 0.020)	0.559 (± 0.029)
Previous Research	DeepDSC	-	0.713 (± 0.014)	0.783 (± 0.009)	0.751 (± 0.011)	0.807 (± 0.009)	0.599 (± 0.021)
	MOFGCN	-	0.492 (± 0.000)	0.666 (± 0.000)	0.355 (± 0.000)	0.650 (± 0.000)	0.901 (± 0.000)
Ablation w/o IP layer	GAT	-	0.758 (± 0.019)	0.868 (± 0.013)	0.703 (± 0.007)	0.687 (± 0.011)	0.395 (± 0.066)
	GT	-	0.774 (± 0.019)	0.874 (± 0.016)	0.717 (± 0.020)	0.717 (± 0.019)	0.566 (± 0.034)
	GINE	-	0.750 (± 0.019)	0.794 (± 0.014)	0.700 (± 0.018)	0.670 (± 0.018)	0.336 (± 0.037)
GraphPINE	GAT	Node Importance	0.789 (± 0.006)	0.892 (± 0.005)	0.720 (± 0.012)	0.717 (± 0.013)	0.547 (± 0.048)
	GT	Node Importance	0.796 (± 0.006)	0.894 (± 0.001)	0.724 (± 0.005)	0.719 (± 0.006)	0.548 (± 0.019)
	GINE	Node Importance	0.790 (± 0.003)	0.891 (± 0.001)	0.730 (± 0.012)	0.728 (± 0.015)	0.575 (± 0.056)

Table 1: Predictive Performance Comparison for Binary Classification. Results show averages of 5 independent runs with standard deviations in parentheses. The best values for each metric are in **bold**. Abbreviations: ROC-AUC: Receiver Operating Characteristic Area Under the Curve, PR-AUC: Precision-Recall Area Under the Curve, RF: Random Forest, MLP: Multiple Layer Perceptron, MPNN: Message-Passing Neural Network, GCN: Graph Convolutional Networks, MOFGCN: Multi-Omics Data Fusion and Graph Convolution Network, GAT: Graph Attention Network, GT: Graph Transformer, GINE: Graph Isomorphism Network with Edge features. Feature Importance: A measure of how much each feature contributes to a model’s predictions.

9-Methoxycamptothecin-Related Gene Interaction Network

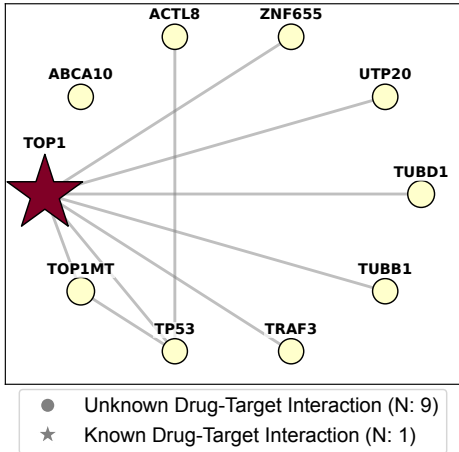


Figure 2: Gene importance scores for 9-Methoxycamptothecin. Node size describes the propagated gene importance, and node color shows the initial DTI score.

Rank	Initial Importance	Gene	PMIDs	Relationship
1	1	TOP1	29312794...	Target
2	-	TOP1MT	24890608...	Indirect
3	-	TUBD1	-	-
4	-	ZNF655	-	-
5	-	UTP20	-	-
6	-	TUBB1	-	-
7	-	ACTL8	-	-
8	-	ABCA10	10606239	Indirect
9	-	TRAF3	-	-
10	-	TP53	12082016...	Indirect

Table 2: Top 10 predicted important genes for 9-Methoxycamptothecin and related literature. (-) represents no initial DTI (0), and (...) describes multiple papers. Target: Genes encoding proteins that directly bind to and interact with the drug. Indirect: Genes that do not encode proteins that physically interact with the drug but are involved in its mechanism of action, pathway, or response.

4.3 INTERPRETABILITY ANALYSIS

GraphPINE assigns importance scores to each gene, indicating their relative significance in predicting drug responses. Figure 2 illustrates the gene interaction network associated with 9-Methoxycamptothecin (MCPT), a DNA damage-related anticancer drug and derivative of camptothecin (CPT). In this network, the size of each node reflects the propagated gene importance after prediction, while the node shape differentiates between known DTIs (denoted by a star) and unknown interaction partners (denoted by a circle). The color of the nodes represents known DTI scores. The

known target of 9-MCPT is TOP1; other genes may affect response directly or indirectly. Figure 2 shows that the known target, TOP1, has the highest DTI score and propagated importance, and other genes have propagated importance but are low compared with TOP1. ABCA10 lacks an edge because it is not among the top interactions shown.

Table 2 lists the top 10 important predictive genes related to 9-MCPT, including TOP1. Although TOP1MT is not known as a target of 9-MCPT, CPT and CPT derivatives can trap TOP1MT-DNA cleavage complexes (Zhang & Pommier, 2008), suggesting 9-MCPT may be indirectly effective against TOP1MT. Additionally, there is an established association between CPT and ABC transporters, making it plausible that ABCA10 might also be related to 9-MCPT activity. Moreover, the efficacy of 9-MCPT may be influenced by the status of TP53, which modulates cellular responses to DNA damage (Abuetaab et al., 2022).

These results demonstrate that GraphPINE can identify biologically relevant gene relationships from gene-gene networks by incorporating prior DTI information. While TOP1MT and TP53 are established as functionally related genes but not known drug targets, our model captures several of these secondary relationships, highlighting its ability to detect both direct and indirect drug-gene associations.

4.4 EVALUATION OF IMPORTANCE SCORE PROPAGATION

To understand the extent to which our importance propagation affects our initial importance scores, we analyzed 6000 randomly selected drug-cell combinations (389 unique drugs \times 26 cell lines) across 5181 genes. Our prior knowledge interaction data is highly sparse; each drug was associated with between 1 and 956 interactors (an average of 39.86 interactions). Appendix B.4 includes a distribution of the number of interactions (Table 3). Importance scores of 0 imply the absence of an interaction, and non-zero values imply an interaction. Therefore, we first examine the extent to which our propagation method increased non-zero values. We observed that non-zero values increased from 0.77% to 39.8% after propagation; this increased the average number of non-zero values per drug from 39.86 to 2061.81 (Appendix B.4). Next, we examined how much individual non-zero values were altered by propagation using a similarity comparison and a rank change analysis. For the similarity analysis (using cosine similarity and Spearman rank correlation), we observe a high but not perfect correlation (0.89 and 0.82, respectively); this suggests importance values that are updated as part of the training process. Approximately 90% of importance values showed some rank change as an effect of propagation with an average shift of ± 67.02 (maximum +946/-932). Next, we considered the situation of starting with random initial importance values, and asked if training shifts these values toward our prior knowledge-derived importance values.

Metric	Value
Cosine sim.	0.87
Spearman corr.	0.82
Rank changes	90.42%
Avg. shift	± 67.02
Max up	946
Max down	-932

Table 3: Differences in Node (Gene) Ranks Before and After Propagation. Cosine sim.: Cosine similarity between initial/propagated importance rank. Spearman corr.: Spearman Rank correlation between initial/propagated importance rank. Rank changes: The percentage of genes whose ranks changed after propagation. Avg. shift: The average rank shift. Max up/down: Maximum upward/downward rank mobility.

5 DISCUSSION

We introduced GraphPINE, an interpretable GNN architecture featuring an ‘‘Importance Propagation Layer’’. Equations 2 through 7 show how node features and importance scores are updated through training while preserving prior knowledge for stability and adaptability.

Our analysis demonstrates that GraphPINE effectively balances initial knowledge with learned patterns. While the model starts with initial node importance values, the propagation mechanism successfully discovers new relationships (increasing interactions from 0.77% to 39.8%) while maintaining meaningful initial characteristics (0.9 cosine similarity). This balance enables both stability

from prior knowledge and adaptability to new patterns. Future work could explore additional information sources, such as protein-protein interaction networks, to further enhance this capability.

While our study focuses on DRP, the GraphPINE framework holds potential for a wide range of applications in fields that involve complex network structures with inherent node importance. For instance, PageRank scores could be used as initial importance values to enhance the propagation of search relevance among web pages in graph analysis.

6 FUNDING

This research was supported in part by the Division of Intramural Research (DIR) of the National Library of Medicine (NLM, ZIALM240126), National Institutes of Health (NIH) (ZIALM240126).

REFERENCES

- Samira Abnar and Willem Zuidema. Quantifying attention flow in transformers. *arXiv preprint arXiv:2005.00928*, 2020.
- Yasser Abuetaf, H Helena Wu, Chengsen Chai, Habib Al Yousef, Sujata Persad, Consolato M Sergi, and Roger Leng. Dna damage response revisited: the p53 family and its regulators provide endless cancer therapy opportunities. *Experimental & molecular medicine*, 54(10):1658–1669, 2022.
- George Adam, Ladislav Rampásek, Zhaleh Safikhani, Petr Smirnov, Benjamin Haibe-Kains, and Anna Goldenberg. Machine learning approaches to drug response prediction: challenges and recent progress. *NPJ precision oncology*, 4(1):19, 2020.
- Takuya Akiba, Shotaro Sano, Toshihiko Yanase, Takeru Ohta, and Masanori Koyama. Optuna: A next-generation hyperparameter optimization framework. In *Proceedings of the 25th ACM SIGKDD International Conference on Knowledge Discovery & Data Mining*, pp. 2623–2631, 2019.
- Francisco Azuaje. Computational models for predicting drug responses in cancer research. *Briefings in Bioinformatics*, 18(5):820–829, 2017.
- Ethan G Cerami, Benjamin E Gross, Emek Demir, Igor Rodchenkov, Özgün Babur, Nadia Anwar, Nikolaus Schultz, Gary D Bader, and Chris Sander. Pathway commons, a web resource for biological pathway data. *Nucleic acids research*, 39(suppl_1):D685–D690, 2010.
- Allan Peter Davis, Cynthia J Grondin, Robin J Johnson, Daniela Sciaky, Jolene Wieggers, Thomas C Wieggers, and Carolyn J Mattingly. The comparative toxicogenomics database (ctd): update 2023. *Nucleic Acids Research*, 51(D1):D1193–D1199, 2023.
- Sharon L Freshour, Susanna Kiwala, Kelsy C Cotto, Adam C Coffman, Joshua F McMichael, Jonathan J Song, Malachi Griffith, Obi L Griffith, and Alex H Wagner. Dgidb 4.0: linking drug–gene interactions with disease associations and functional impact. *Nucleic Acids Research*, 49(D1): D1334–D1342, 2021.
- Tianfan Fu, Wenhao Gao, Cao Xiao, Jacob Yasonik, Connor W Coley, and Jimeng Sun. Differentiable scaffolding tree for molecular optimization. *arXiv preprint arXiv:2109.10469*, 2021a.
- Tianfan Fu, Cao Xiao, Xinhao Li, Lucas M Glass, and Jimeng Sun. Mimosa: Multi-constraint molecule sampling for molecule optimization. In *Proceedings of the AAAI Conference on Artificial Intelligence*, volume 35, pp. 125–133, 2021b.
- Justin Gilmer, Samuel S Schoenholz, Patrick F Riley, Oriol Vinyals, and George E Dahl. Neural message passing for quantum chemistry. In *International conference on machine learning*, pp. 1263–1272. PMLR, 2017.
- Weihua Hu, Bowen Liu, Joseph Gomes, Marinka Zitnik, Percy Liang, Vijay Pande, and Jure Leskovec. Strategies for pre-training graph neural networks. *arXiv preprint arXiv:1905.12265*, 2019.
- Kexin Huang, Tianfan Fu, Wenhao Gao, Yue Zhao, Yusuf Roohani, Jure Leskovec, Connor W Coley, Cao Xiao, Jimeng Sun, and Marinka Zitnik. Therapeutics data commons: Machine learning datasets and tasks for drug discovery and development. *arXiv preprint arXiv:2102.09548*, 2021.
- Yoshitaka Inoue, Hunmin Lee, Tianfan Fu, and Augustin Luna. drgat: Attention-guided gene assessment of drug response utilizing a drug-cell-gene heterogeneous network. *arXiv preprint arXiv:2405.08979*, 2024.
- Guolin Ke, Qi Meng, Thomas Finley, Taifeng Wang, Wei Chen, Weidong Ma, Qiwei Ye, and Tie-Yan Liu. Lightgbm: A highly efficient gradient boosting decision tree. *Advances in neural information processing systems*, 30, 2017.
- Thomas N Kipf and Max Welling. Semi-supervised classification with graph convolutional networks. *arXiv preprint arXiv:1609.02907*, 2016.

- Johannes Klicpera, Stefan Weissenberger, and Stephan Günnemann. Diffusion improves graph learning. In *Advances in Neural Information Processing Systems*, volume 32, 2019.
- Viet Dac Lai, Tuan Ngo Nguyen, and Thien Huu Nguyen. Event detection: Gate diversity and syntactic importance scores for graph convolution neural networks, 2020.
- Chuanqi Lao, Pengfei Zheng, Hongyang Chen, Qiao Liu, Feng An, and Zhao Li. Deepaeg: a model for predicting cancer drug response based on data enhancement and edge-collaborative update strategies. *BMC bioinformatics*, 25(1):105, 2024.
- Min Li, Yake Wang, Ruiqing Zheng, Xinghua Shi, Yaohang Li, Fang-Xiang Wu, and Jianxin Wang. Deepdsc: a deep learning method to predict drug sensitivity of cancer cell lines. *IEEE/ACM transactions on computational biology and bioinformatics*, 18(2):575–582, 2019.
- Yingzhou Lu. *Multi-omics Data Integration for Identifying Disease Specific Biological Pathways*. PhD thesis, Virginia Tech, 2018.
- Augustin Luna, Vinodh N Rajapakse, Fabricio G Sousa, Jianjiong Gao, Nikolaus Schultz, Sudhir Varma, William Reinhold, Chris Sander, and Yves Pommier. rcellminer: exploring molecular profiles and drug response of the nci-60 cell lines in r. *Bioinformatics*, 32(8):1272–1274, 2016.
- Scott M Lundberg and Su-In Lee. A unified approach to interpreting model predictions. *Advances in neural information processing systems*, 30, 2017.
- Tuan Nguyen, Giang TT Nguyen, Thin Nguyen, and Duc-Hau Le. Graph convolutional networks for drug response prediction. *IEEE/ACM transactions on computational biology and bioinformatics*, 19(1):146–154, 2021.
- Wei Peng, Tielin Chen, and Wei Dai. Predicting drug response based on multi-omics fusion and graph convolution. *IEEE Journal of Biomedical and Health Informatics*, 26(3):1384–1393, 2021.
- Igor Rodchenkov, Ozgun Babur, Augustin Luna, Bulent Arman Aksoy, Jeffrey V Wong, Dylan Fong, Max Franz, Metin Can Siper, Manfred Cheung, Michael Wrana, Harsh Mistry, Logan Mosier, Jonah Dlin, Qizhi Wen, Caitlin O’Callaghan, Wanxin Li, Geoffrey Elder, Peter T Smith, Christian Dallago, Ethan Cerami, Benjamin Gross, Ugur Dogrusoz, Emek Demir, Gary D Bader, and Chris Sander. Pathway Commons 2019 Update: integration, analysis and exploration of pathway data. *Nucleic Acids Research*, 48(D1):D489–D497, 10 2019. ISSN 0305-1048. doi: 10.1093/nar/gkz946. URL <https://doi.org/10.1093/nar/gkz946>.
- Eric Sayers. The e-utilities in-depth: parameters, syntax and more. *Entrez Programming Utilities Help [Internet]*, 2009.
- Ramprasaath R Selvaraju, Michael Cogswell, Abhishek Das, Ramakrishna Vedantam, Devi Parikh, and Dhruv Batra. Grad-cam: visual explanations from deep networks via gradient-based localization. *International journal of computer vision*, 128:336–359, 2020.
- Robert H Shoemaker. The nci60 human tumour cell line anticancer drug screen. *Nature Reviews Cancer*, 6(10):813–823, 2006.
- Avanti Shrikumar, Peyton Greenside, and Anshul Kundaje. Learning important features through propagating activation differences. *arXiv preprint arXiv:1704.02685*, 2017.
- Damian Szklarczyk, Alberto Santos, Christian von Mering, Lars Juhl Jensen, Peer Bork, and Michael Kuhn. Stitch 5: augmenting protein–chemical interaction networks with tissue and affinity data. *Nucleic Acids Research*, 49(D1):D467–D474, 2021.
- Jing Tang, Agnieszka Sz wajda, Sushil Shakyawar, Tao Xu, Petteri Hintsanen, Krister Wennerberg, and Tero Aittokallio. Making sense of large-scale kinase inhibitor bioactivity data sets: a comparative and integrative analysis. *Journal of Chemical Information and Modeling*, 54(3):735–743, 2014.
- Jessica Vamathevan, Dominic Clark, Paul Czodrowski, Ian Dunham, Edgardo Ferran, George Lee, Bin Li, Anant Madabhushi, Parantu Shah, Michaela Spitzer, et al. Applications of machine learning in drug discovery and development. *Nature Reviews Drug Discovery*, 18(6):463–477, 2019.

- Petar Veličković, Guillem Cucurull, Arantxa Casanova, Adriana Romero, Pietro Lio, and Yoshua Bengio. Graph attention networks. *arXiv preprint arXiv:1710.10903*, 2017.
- Yue Wang, Tianfan Fu, Yinlong Xu, Zihan Ma, Hongxia Xu, Bang Du, Yingzhou Lu, Honghao Gao, Jian Wu, and Jintai Chen. Twin-gpt: Digital twins for clinical trials via large language model. *ACM Transactions on Multimedia Computing, Communications and Applications*, 2024.
- David S Wishart, Yannick D Feunang, An C Guo, Elvis J Lo, Ana Marcu, Jason R Grant, Tanvir Sajed, Daniel Johnson, Carin Li, Zinat Sayeeda, et al. Drugbank 5.0: a major update to the drugbank database for 2018. *Nucleic Acids Research*, 46(D1):D1074–D1082, 2018.
- Rex Ying, Dylan Bourgeois, Jiaxuan You, Marinka Zitnik, and Jure Leskovec. Gnnexplainer: Generating explanations for graph neural networks. In *Advances in neural information processing systems*, volume 32, 2019.
- Seongjun Yun, Minbyul Jeong, Raehyun Kim, Jaewoo Kang, and Hyunwoo J Kim. Graph transformer networks. In *Advances in Neural Information Processing Systems*, volume 32, 2019.
- Daojian Zeng, Chao Zhao, and Zhe Quan. Cid-gcn: an effective graph convolutional networks for chemical-induced disease relation extraction. *Frontiers in Genetics*, 12:624307, 2021.
- Hongliang Zhang and Yves Pommier. Mitochondrial topoisomerase i sites in the regulatory d-loop region of mitochondrial dna. *Biochemistry*, 47(43):11196–11203, 2008.
- Marinka Zitnik, Monica Agrawal, and Jure Leskovec. Modeling polypharmacy side effects with graph convolutional networks. *Bioinformatics*, 34(13):i457–i466, 2018.

A IMPLEMENTATION DETAILS AND HYPERPARAMETER TUNING

A.1 DATA PREPROCESSING AND NETWORK CONSTRUCTION

We integrated multiple data sources to create a comprehensive gene-gene interaction network and DTI dataset. Our approach involves several key steps.

A.1.1 DATA INTEGRATION

Let $G = g_1, g_2, \dots, g_n$ be the set of all genes, and $D = d_1, d_2, \dots, d_m$ be the set of all drugs. We collected data from various sources. From NCI-60 cell lines, we obtained multi-omics data including gene expression ($X_{exp} \in \mathbb{R}^{n \times c}$), methylation ($X_{met} \in \mathbb{R}^{n \times c}$), mutation ($X_{mut} \in \{0, 1\}^{n \times c}$), and copy number variation (CNV) ($X_{cnv} \in \mathbb{R}^{n \times c}$), where n is the number of genes and c is the number of cell lines. Gene-gene interaction data ($E_{gg} \subseteq G \times G$) was sourced from PathwayCommons (Cerami et al., 2010; Rodchenkov et al., 2019), containing various types of interactions such as catalysis-precedes, controls-expression-of, controls-phosphorylation-of, controls-state-change-of, controls-transport-of, in-complex-with, and interacts-with. DTI data ($E_{dti} \subseteq D \times G$) was collected from multiple sources, including the CTD, DrugBank, DGIdb, STITCH, and the KIBA dataset.

A.1.2 GENE-GENE NETWORK CONSTRUCTION

We selected a subset of genes $G' \subseteq G$ based on three criteria. (1) First, we considered variance in multi-omics data. For each data source $s \in \{\text{exp}, \text{met}, \text{mut}, \text{cnv}\}$ where exp represents gene expression, met represents methylation, mut represents mutation, and cnv represents copy number variation, we computed the variance for each gene across cell lines:

$$\text{var}_s(g_i) = \frac{1}{c-1} \sum_{j=1}^c (X_{s_{ij}} - \bar{X}_{s_i})^2 \quad (10)$$

We selected the top 3000 genes with the highest variance for each data source. (2) Second, we computed network centrality, calculating the degree of centrality for each gene in the initial interaction network:

$$\text{centrality}(g_i) = \frac{|(g_i, g_j) \in E_{gg} \vee (g_j, g_i) \in E_{gg}|}{|G| - 1} \quad (11)$$

We selected the top 3000 genes with the highest centrality. (3) Third, we considered DTI frequency, calculating the frequency of each gene in the DTI data:

$$\text{freq}_{dti}(g_i) = |(d_j, g_i) \in E_{dti}| \quad (12)$$

We selected the top 3000 genes with the highest DTI frequency. The final set of genes G' was the union of these selections, resulting in 5,181 genes. We then constructed the gene-gene interaction network $G' = (V', E')$, where $V' = G'$ and $E' = E_{gg} \cap (G' \times G')$, containing 630,632 interactions.

A.1.3 EDGE ENCODING

Each interaction between genes is categorized into one of seven types based on the information from PathwayCommons: “catalysis-precedes”, “controls-expression-of”, “controls-phosphorylation-of”, “controls-state-change-of”, “controls-transport-of”, “in-complex-with”, and “interacts-with”. These interaction types were encoded as one-hot vectors.

Let $T = \{t_1, t_2, \dots, t_7\}$ represent the set of all interaction types. For each edge $e \in E'$, a binary vector $v_e \in \{0, 1\}^7$ was created, where each element corresponds to a specific interaction type:

$$v_e[i] = \begin{cases} 1 & \text{if edge } e \text{ has interaction type } t_i \\ 0 & \text{otherwise.} \end{cases} \quad (13)$$

A.1.4 MULTI-OMICS DATA PREPROCESSING

We focused on normalizing gene expression data through several steps. First, we converted the data to Transcripts Per Million (TPM):

$$\text{TPM}_{ij} = \frac{X_{\text{exp}_{ij}}}{\sum_{i=1}^n X_{\text{exp}_{ij}}} \times 10^6. \quad (14)$$

Next, we applied a Log2 transformation:

$$X'_{\text{exp}_{ij}} = \log_2(\text{TPM}_{ij} + 1). \quad (15)$$

Finally, we performed Winsorization. Let $q_{0.1}$ and $q_{99.9}$ be the 0.1 and 99.9 percentiles of X'_{exp} . We applied:

$$X''_{\text{exp}_{ij}} = \begin{cases} q_{0.1} & \text{if } X'_{\text{exp}_{ij}} < q_{0.1} \\ q_{99.9} & \text{if } X'_{\text{exp}_{ij}} > q_{99.9} \\ X'_{\text{exp}_{ij}} & \text{otherwise.} \end{cases} \quad (16)$$

These steps ensured our gene expression data was normalized and scaled for further analysis. We then created 4-dimensional feature vectors for each gene in each cell line:

$$X_i = [X''_{\text{exp}_i}, X_{\text{met}_i}, X_{\text{mut}_i}, X_{\text{cnv}_i}]. \quad (17)$$

A.2 IMPLEMENTATION DETAILS

The GraphPINE model was implemented using Python 3.10, PyTorch 2.4.0, and PyTorch Geometric 2.5.3, leveraging their efficient deep learning and graph processing capabilities. We employed the Adam optimizer for training, with a learning rate of 0.001 and a batch size of 32. The model architecture incorporates 3 Importance Propagation Layers ($L = 3$), each containing 64 hidden units. To balance model performance and interpretability, we set the importance regularization coefficient λ to 0.01 and the importance threshold τ to 0.1.

All experiments were conducted on NVIDIA Tesla A100 GPUs with 80 GB memory. The average training time for GraphPINE was 0.2 seconds, with an inference time of 0.1 seconds per drug-cell line pair, demonstrating its feasibility for large-scale DRP tasks. To ensure reproducibility and facilitate further research, we have made our code and datasets publicly available at <https://anonymous.4open.science/r/GraphPINE-40DE>.

A.3 TRAINING PROCEDURE

The training procedure for the GraphPINE model is designed to optimize performance while preventing overfitting. Algorithm 1 presents a detailed overview of this process. Concretely, the GraphPINE training procedure involves initializing model parameters, iterating through epochs, performing forward and backward passes, computing losses, and updating parameters. The procedure also includes an early stopping mechanism to prevent overfitting.

We employ the Adam optimizer with an initial learning rate of $\eta = 10^{-3}$.

A.4 HYPERPARAMETER TUNING

To optimize the performance of our GraphPINE model, we conducted extensive hyperparameter tuning using Optuna (Akiba et al., 2019), an efficient hyperparameter optimization framework. We utilized MLflow for experiment tracking and logging, ensuring comprehensive documentation of our optimization process.

Our hyperparameter search space encompassed key model parameters, including the number of epochs (1-3), number of attention heads (1, 2, 4), number of GNN layers (2-4), dropout rate (0.1-0.3), importance decay (0.7-0.9), importance threshold (1e-5 to 1e-3), hidden channel size (16, 32), BCE weight (0.9-1.1), importance regularization weight (0.005-0.02), and learning rate (0.001-0.1). The batch size was initially set to 5, with a dynamic reduction mechanism implemented to handle potential memory constraints.

The optimization process consisted of 20 trials, each involving the following steps: (1) hyperparameter suggestion by Optuna, (2) GraphPINE model initialization with the suggested configuration, (3) model training and validation, and (4) reporting of the minimum validation loss as the objective value for optimization. This systematic approach allowed us to identify the optimal hyperparameter configuration that balanced model performance and computational efficiency.

Algorithm 1 GraphPINE Training Procedure

```

1: Initialize model parameters  $\theta$ 
2: Initialize optimizer with learning rate  $\eta$ 
3: Set early stopping patience  $p$  and minimum delta  $\delta$ 
4: for epoch = 1 to  $T_{\text{total}}$  do
5:   for batch in training data do
6:     Forward pass:  $\hat{y}, I' = f_{\theta}(X, E, I)$ 
7:     Compute loss:  $L = w_{\text{BCE}} \cdot \mathcal{L}_{\text{BCE}}(\hat{y}, y) + w_{\text{imp}} \cdot \mathcal{L}_{\text{imp}}(I', I)$ 
8:     Backward pass: Compute  $\nabla_{\theta} \mathcal{L}$ 
9:     Update parameter using Adam optimizer.
10:  end for
11:  Evaluate on the validation set
12:  if validation loss improved by at least  $\delta$  then
13:    Reset patience counter
14:    Save the best model
15:  else
16:    Decrement patience counter
17:    if patience counter = 0 then
18:      Early stop and return best model
19:    end if
20:  end if
21: end for

```

Throughout the implementation and tuning process, we leveraged several key libraries and tools. PyTorch served as the foundation for building and training our neural network model. Optuna facilitated efficient hyperparameter optimization, while MLflow provided robust experiment tracking and logging capabilities. We also utilized NumPy for numerical computations and Pandas for data manipulation and analysis, ensuring a comprehensive and efficient development environment.

This rigorous implementation and tuning process enabled us to develop a highly optimized GraphPINE model capable of accurate and interpretable DRPs. The combination of advanced deep learning techniques, efficient hyperparameter optimization, and careful implementation considerations resulted in a model that balances performance, interpretability, and computational efficiency.

A.5 BASELINE SETTING

We implemented three baseline models for comparison: Random Forest (RF), LightGBM, and Multiple Layer Perceptron (MLP). All models were trained on the same dataset, which combined gene expression, methylation, mutation, copy number variation, and drug-target interaction data.

Random Forest (RF): We used `scikit-learn`'s `RandomForestClassifier` with hyperparameters optimized via `Optuna`. The key hyperparameters included the number of estimators (100–1000), max depth (10–100), min samples split (2–20), min samples leaf (1–10), and max features (None, "sqrt", or "log2").

LightGBM: We implemented LightGBM (Ke et al., 2017) with binary classification objective and log loss metric. Hyperparameters were tuned using `Optuna`, including `num_leaves` (31–255), `learning_rate` (1e-3 to 1.0), `feature_fraction` (0.1–1.0), `bagging_fraction` (0.1–1.0), `bagging_freq` (1–7), `min_child_samples` (5–100), `lambda_l1` and `lambda_l2` (1e-8 to 10.0), and `num_boost_round` (100–2000).

Multiple Layer Perceptron (MLP): We created a `PyTorch`-based MLP with a flexible architecture. Hyperparameters optimized via `Optuna` included the number of layers (2–5), hidden dimensions (64–512 units per layer), learning rate (1e-5 to 1e-1), batch size (32, 64, 128, or 256), dropout rate (0.1–0.5), and normalization type (batch or layer normalization).

DeepDSC and MOFGCN: For DeepDSC, we follow the original architecture consisting of a stacked autoencoder followed by a feed-forward network. The encoder comprises three hidden layers (2,000, 1,000, and 500 units), while the decoder mirrors this with hidden layers of 1,000 and 2,000 units. The activation function is selu for hidden layers and sigmoid for the output layer. Training employs AdaMax optimizer with a learning rate of 0.0001, gradient clipping at 1.0, and Xavier uniform initialization¹.

For MOFGCN, we utilize the following hyperparameters: scale parameter $\varepsilon = 2$, proximity parameter $N = 11$, number of iterations $t = 3$, embedding dimension $h = 192$, correlation information dimension $k = 36$, scaling parameter $\alpha = 5.74$, learning rate 5×10^{-4} , and 1000 training epochs. The model uses the PyTorch framework with Adam optimizer.

Both models employ early stopping to prevent overfitting - DeepDSC with the patience of 30 epochs and MOFGCN monitoring the validation loss.

MPNN, GCN, and GINE: For the MPNN (Message-Passing Neural Network) (Gilmer et al., 2017), GCN (Graph Convolutional Network) (Kipf & Welling, 2016), and GINE (Graph Isomorphism Network with Edge features) (Hu et al., 2019), we tuned the hyperparameters using the following configuration. The number of epochs (num_epochs) was selected from {10, 50, 100}. The batch size was chosen from {2, 3, 4}. The number of GNN layers was selected from {1, 2, 3}. The dropout rate was selected from {0.1, 0.2, 0.3}. The importance decay was chosen from {0.7, 0.8, 0.9}. The importance threshold was selected from {1e-5, 1e-4, 1e-3}. The hidden channel size was selected from {16, 32}. The weight for the mean squared error loss was selected from {0.9, 1.0, 1.1}. The weight for importance regularization was selected from {0.005, 0.01, 0.02}. The learning rate was selected from {0.001, 0.01, 0.1}.

GAT and Graph Transformer: For the GAT (Graph Attention Network) (Veličković et al., 2017) and Graph Transformer models (Yun et al., 2019), we used a similar hyperparameter tuning configuration as for MPNN, GCN, and GINE. However, for GAT and Graph Transformer, we also included the number of attention heads, which was selected from {1, 2, 4}. This additional parameter helps in controlling the number of attention mechanisms in the model, enabling it to learn more complex representations.

For all models, we used Optuna for hyperparameter optimization, maximizing accuracy on the validation set. Each model was then trained five times with the best hyperparameters, and we reported the mean and standard deviation of accuracy, precision, recall, and F1 score on the test set.

The data preprocessing steps were consistent across all models, including normalization of gene expression data and concatenation of multi-omics features. This ensured a fair comparison between the baseline models and our proposed GraphPINE method.

B EXPERIMENTS

B.1 DATASET AND PREPROCESSING

In this study, we utilized a comprehensive drug response dataset containing information on multiple cell lines and compounds. The dataset was preprocessed and split to ensure a rigorous evaluation of the model’s generalization capabilities. Initially, the dataset contained IC50 data for unique cell lines and unique NSC (Cancer Chemotherapy National Service Center number) identifiers for compounds.

To adapt this data for binary classification, we applied an empirically determined threshold, which was set to achieve an approximately 50:50 ratio of response to non-response using the formula below.

$$\text{binarize}(x) = \begin{cases} 1 & \text{if } x < \text{threshold} \\ 0 & \text{otherwise,} \end{cases}, \quad (18)$$

where the threshold is the hyperparameter, and we set -4.595.

This process resulted in a dataset of 331,558 entries. We then refined our dataset to focus on the 60 cell lines present in the NCI60 panel, reducing the data to 315,778 entries. Further narrowing our scope to include only the drugs used in the NCI60 project, we arrived at a final dataset of 53,852 entries.

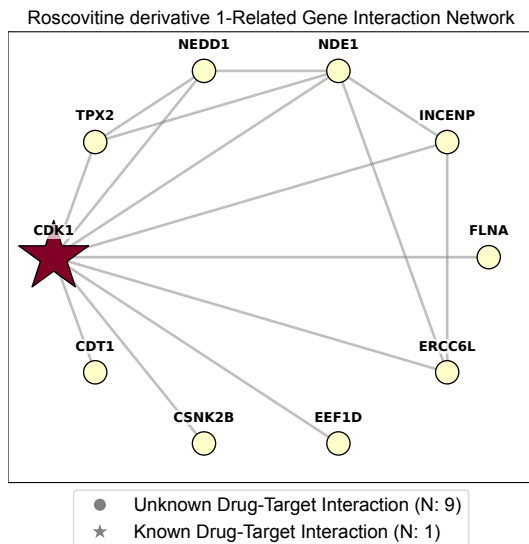


Figure 3: Gene importance scores and interactions for Roscovitine derivative 1. Node size describes the propagated gene importance.

Table 4: Top 10 predicted important genes for Roscovitine derivative 1.

Rank	Gene Name	Evidence (PMID)
1	CDK1	37635245
2	NDE1	-
3	INCENP	-
4	EEF1D	-
5	NEDD1	-
6	CDT1	35931300
7	CSNK2B	-
8	TPX2	-
9	ERCC6L	-
10	FLNA	-

To set up a zero-shot prediction scenario, we randomly selected 70% of unique cell lines and 60% of unique NSC identifiers for the training and validation sets. The remaining cell lines and NSC identifiers were used for the test set, ensuring no overlap of cell lines or compounds between the train/validation and test sets. This approach allows us to evaluate the model’s ability to generalize to entirely new cell-compound combinations.

The data was split as follows: The training set comprises 18,067 entries, consisting of 571 unique drugs (NSCs) and 42 unique cell lines. The validation set contains 4,516 entries, utilizing the same 571 drugs and 42 cell lines as the training set. The test set includes 6,525 entries, encompassing 381 unique drugs and 18 unique cell lines.

Notably, while the training and validation sets share common cell lines and drugs, the test set introduces new drug-cell line combinations. This configuration allows for a rigorous assessment of our model’s generalization capability, enabling us to evaluate its predictive performance on unseen drug-cell line pairs.

B.2 EVALUATION METRICS

We evaluated GraphPINE using a comprehensive set of metrics to assess its classification performance. The Accuracy was used to measure the overall correctness of the model’s predictions across all classes. To provide a more nuanced assessment of the model’s discriminative ability, we calculated the Area Under the Receiver Operating Characteristic curve (ROC-AUC) and the Area Under the Precision-Recall curve (PR-AUC). ROC-AUC quantifies the model’s ability to distinguish between classes across various threshold settings, while PR-AUC is particularly useful for evaluating performance on imbalanced datasets. To further characterize the model’s performance on negative instances, we computed the Specificity, which measures the proportion of actual negatives correctly identified. Additionally, we calculated the Negative Predictive Value (NPV), which quantifies the proportion of negative predictions that were correct. These metrics collectively offer a thorough evaluation of GraphPINE’s ability to correctly classify both positive and negative instances, providing insights into its performance across different aspects of the classification task.

B.3 INTERPRETABILITY ANALYSIS

Figure 3 shows the predicted interaction network for a roscovitine derivative. The network contains mostly unknown interactions (9) with only one known interaction. CDK1 is highlighted as the most

important predicted target gene. This suggests the roscovitine derivative may have new mechanisms of action beyond the known CDK inhibition, but CDK1 remains a key target.

Table 4 lists the top 10 predicted important genes for the roscovitine derivative. CDK1 is ranked first, consistent with roscovitine’s known mechanism as a CDK inhibitor. However, most other predicted genes, like NDE1, INCENP, EEF1D, etc. are new interactions without existing evidence. This suggests potential new pathways the derivative may affect beyond CDK inhibition.

B.4 EVALUATION OF IMPORTANCE SCORE PROPAGATION

To validate our important propagation mechanism’s effectiveness, we analyzed rank comparisons before/after propagation across 6000 randomly selected drug-cell combinations (389 unique drugs, 26 unique cell lines) and 5181 genes.

The initial importance density was 0.77% with an average of 39.86 interactions per drug-cell combination. After propagation, the interaction density increased to 39.8% (+38.96%) with 2061.81 average interactions.

The metrics comparison revealed a high cosine similarity of 0.9, indicating that 90% of genes maintained their original characteristics post-propagation. While the overall Spearman rank correlation was low due to zero entries, non-zero entries showed a strong correlation of 0.81, confirming the preservation of meaningful relationships during network expansion.

99.98% of genes showed rank changes, with an average shift of ± 1156.82 positions (maximum: +2658, minimum: -2590). This substantial change, combined with high similarity (0.90) to the original data, indicates the successful discovery of hidden connections while maintaining data integrity.

For non-zero DTI entries specifically, 90.5% of genes changed ranks with an average shift of ± 69.71 (maximum: +946, minimum: -932). This demonstrates that our model modifies rankings for both zero and non-zero entries while preserving cosine similarity and rank correlation.

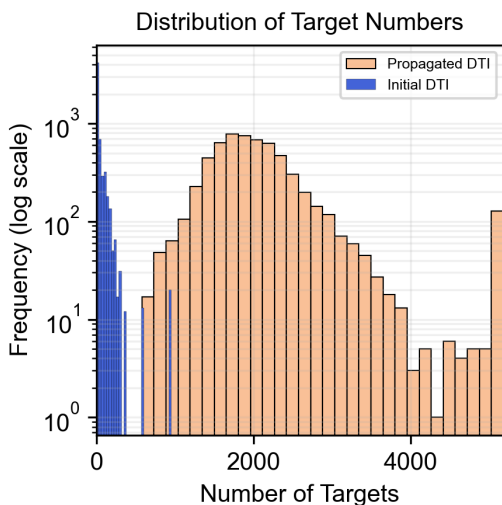


Figure 4: Distribution of Interactions Numbers Before/After Propagation. Initial interactions (blue) show a concentrated distribution near zero interactions, while Propagated interactions (orange) demonstrate a broader distribution centered around 2000 interactions.